Bioorganic & Medicinal Chemistry 18 (2010) 5754–5761

Contents lists available at ScienceDirect

Bioorganic & Medicinal Chemistry

journal homepage: www.elsevier.com/locate/bmc

Rational conversion of noncontinuous active region in proteins into a small orally bioavailable macrocyclic drug-like molecule: The HIV-1 CD4:gp120 paradigm

Mattan Hurevich [a,*,†], Avi Swed [b,†], Salim Joubran [a], Shira Cohen [a], Noam S. Freeman [a], Elena Britan-Rosich [d], Laurence Briant-Longuet [c], Martine Bardy [c], Christian Devaux [c], Moshe Kotler [d], Amnon Hoffman [b], Chaim Gilon [a,*]

[a] Institute of Chemistry, The Hebrew University of Jerusalem, Edmond Safra Campus, Givat Ram Campus, The Hebrew University, Jerusalem 91904, Israel
[b] Departments of Pharmaceutics, Scholl of Pharmacy, The Hebrew University of Jerusalem, Hadassa Ein Karem Campus, The Hebrew University, Jerusalem 91120, Israel
[c] Institut de Biologie CNRS UMR5121, Laboratoire Infections Retrovirales et Signalisation Cellulaire, CNRS UMR5121, Institut de Biologie, Montpellier 34960, France
[d] Departments of Pathology, Medical Scholl, Hadassa Ein Karem Campus, The Hebrew University, Jerusalem 91120, Israel

ARTICLE INFO

Article history:
Received 8 March 2010
Revised 16 April 2010
Accepted 17 April 2010
Available online 21 April 2010

Keywords:
Backbone cyclization
Drug design
HIV-1
Macrocycles
Proteomics

ABSTRACT

Rational conversion of noncontinuous active regions of proteins into a small orally bioavailable molecule is crucial for the discovery of new drugs based on inhibition of protein–protein interactions. We developed a method that utilizes backbone cyclization as an intermediate step for conversion of the CD4 noncontinuous active region into small macrocyclic molecules. We demonstrate that this method is feasible by preparing small inhibitor for human immunodeficiency virus infection. The lead compound, CG-1, proved orally available in the rat model.

1. Introduction

Protein–protein interactions (PPI) are key players in many intercellular interactions and are involved in many diseases. They are considered as potential targets for drug intervention. However, conversion of active region of proteins into a drug-like molecule is challenging. It is even more problematic when the active pharmacophores are in spatial proximity yet distant in the protein sequence. In these cases only large peptides are considered able to mimic the entire active region. We previously reported a procedure to convert a noncontinuous active region in proteins, comprising few pharmacophors, into a backbone cyclic peptide that mimics the active region of the target protein.[1] Backbone cyclization (BC) is a general method for conversion of peptides into drugable peptidomimetic. In this method conformational constraint is imposed on peptides.[2] The advantage of BC is achieving cyclization mainly by using backbone atoms, thus, avoiding the use of side chains and peptidic ends that are essential for the biological activity. Moreover, backbone cyclization has been shown to impose metabolic stability and intestinal permeability.[3,4] Screening of backbone cyclic libraries with conformational diversity (cycloscan) was used here in order to reduce the size of the active region of CD4 into a small molecule.

Human immunodeficiency virus (HIV-1) entry into the host cell is initially mediated by the interaction of viral envelope proteins with T-cell transmembrane proteins.

CD4 engagement by gp120 is a critical step in virus penetration and its inhibition by drug intervention is the goal of several research groups and pharmaceutical companies.[5] Small molecules

Abbreviations: AcOH, acetic acid; Alloc, allyloxycarbonyl; Boc, *t*-butoxycarbonyl; BTC, *bis*(trichloromethyl)carbonate; DBU, 1,8-diazabicyclo[5.4.0]undec-7-ene; DCM, methylene chloride; DIC, *N*,*N*′-diisopropylcarbodiimide; DIPEA, diisopropylethylamine; DMAP, dimethylaminopyridine; DMF, *N*,*N*′-dimethylformamide; Fmoc, 9-fluorenylmethyloxycarbonyl; HATU, 2-(7-aza-1*H*-benzotriazole-1-yl)-1,1,3,3-tetramethyluronium hexafluorophosphate; HBTU, (2-(1*H*-benzotriazole-1-yl)-1,1,3,3-tetramethyluronium hexafluorophosphate; HIV-1, human immunodeficiency virus; HOAt, 1-hydroxy-7-aza-benzotriazole; IV, intravenous; MAGI, multinuclear activation of a galactosidase indicator; MBHA, 4-methylbenzhydrylamine; NMM, 4-methylmorpholine; PO, per os; PPI, protein–protein interaction; PyClock, 6-chloro-benzotriazole-1-yl-oxy-tris-pyrrolidino-phosphonium hexafluorophosphate; TDW, triple distilled water; TFA, trifluoroacetic acid; TIPS, triisopropylsilane.

* Corresponding authors. Tel.: +972 (0)2 6586 181; fax: +972 (0)2 6416 358 (C.G.).
E-mail address: gilon@vms.huji.ac.il (C. Gilon).
† Both authors contributed equally to this work.

0968-0896/$ - see front matter © 2010 Elsevier Ltd. All rights reserved.
doi:10.1016/j.bmc.2010.04.053

like BMS-806[6] and NBD-556[7] recently showed promising preliminary results while peptide inhibitors like T-20[8] have been commercially available. Although the structure of the CD4:gp120 complex has been previously resolved[9] only few drug candidates were developed in order to target this interaction. This shortcoming can be accounted for the large conformational changes experienced in the viral envelope structure during CD4 binding. These changes influence the Phe43 pocket and the structure of the site in the unbound state is still unclear. Another difficulty in rational design of CD4 mimetic stems from the fact that HIV-1 gp120 binding site in CD4 is noncontinuous. Insertion of mutation into CD4 molecule pointed out that Lys29, Lys35, Phe43, Lys46, and Arg59 residues participate in gp120 binding.[10–13] The CD4 Phe43 is positioned in a type II′ β-turn on the first domain of the extra-cellular part of the protein and is the most significant residue for gp120 binding. The phenylic side chain is involved in numerous interactions with large hydrophobic pocket in gp120. Arg59, which is positioned on an α-helix in close spatial proximity to the above mentioned β-turn also plays a pivotal role in the interaction. Calculations based on the X-ray structure of the CD4:gp120 complex indicate that the mean distance between the two pharmacophores is less than 10 Å. The short distance between the pharmacophores suggests that this site can be mimicked by small molecule and not only by large peptides[14] (Fig. 1).

A rational method for the conversion of a noncontinuous active site in a protein into a small macrocyclic proteinomimetic molecule is described. We applied a backbone cyclic peptide library screening method as an intermediate step for the rational design of CD4 mimetic small anti HIV-1 drug lead based on two important residues. We prepared a macrocyclic molecule that inhibits HIV-1 infection in cells. This molecule has substantial oral bioavailability in animals and shows good distribution in tissues.

2. Results and discussion

2.1. Backbone cyclic HIV-1 inhibitors 1st generation

The in vitro model of CD4 gp120 interaction is unfortunately not well established. Other groups that developed anti HIV-1 entry inhibitors found it hard to prove the exact inhibition mechanism of these drug leads. These works (e.g., Si et al.) suggest that gp120 inhibitors can occupy the hydrophobic pocket without disturbing the interaction with CD4 and can lead to inhibition by inducing conformational changes to gp120. The cellular approach is considered as an efficient alternative to the somewhat indecisive binding assay. We decided to use the direct cell inhibition assay in order to establish the concept of minimization through backbone cyclization.

We synthesized backbone cyclic peptide library (named C-*n*-*m*, for nomenclature Scheme 1) that preserve the two crucial pharmacophores of the CD4 active site (Phe43 and Arg59). To obtain an active backbone cyclic CD4 mimetic, four amino acids comprising the turn around the Phe43 were preserved. In addition, the Arg moiety was introduced as part of the bridge (Scheme 1). Optimization of the distance between the Arg and Phe residues was achieved by gradual addition of one or two methylenes to the *n* or *m* side of the bridge. These systematic changes enabled us to partially scan the conformational space of the scaffold, thus leading to the desired bioactive conformation.

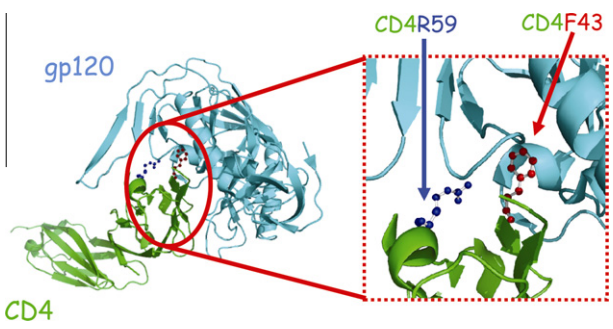

Figure 1. CD4:gp120 complex crystal structure. Blue-Arg59, red-Phe43 two CD4 pharmacophors crucial for the gp120 binding interaction.

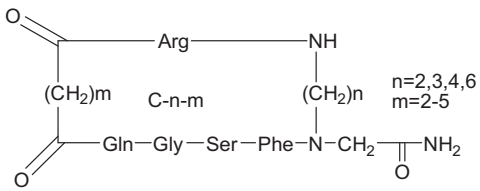

Scheme 1. Structure of the C-*n*-*m* backbone cyclic library. Nomenclature, in the C-*n*-*m* library *n* represents the number of methylenes in the N-alkylated building unit and *m* represents the number of methylenes in the dicarboxylic acid linker.

The effect of backbone cyclic peptides on HIV-1 propagation was studied by using MAGI cells, which express the β-galactosidase gene under transcription activator region regulation.[15] Mock or HIV-1 infected cultured cells show that 100 μM of the cyclic peptide C-2-2 (for structure and nomenclature see Scheme 1 footnote) reduced the viral infectivity by over 80% (Fig. 2). Furthermore, the four peptides, C-2-2, C-2-3, C-2-4, and C-2-5 (all bearing two methylenes in the *n* side) were the most potent inhibitors in the library and reduced infectivity by 84%, 80%, 76%, and 68%, respectively in 100 μM concentrations. Contrary, no distinctive correlation between the inhibitory effect and the *m* size was observed.

Results from the C-*n*-*m* library indicate that the proximity of the Phe moiety to the Arg residue on the *n* side directly affects the efficacy of the CD4 derived cyclic peptides on HIV-1 infectivity. These results suggest that mimicking of the CD4 active site is possible using small backbone cyclic peptides and that the size of the inhibitor can be further reduced.

2.2. Design and synthesis of small molecule macrocyclic HIV-1 infection inhibitors

The straightforward conformational screening of the C-*n*-*m* library drew a pattern which allowed us to design small molecule inhibitors. Our design focused on creating small macrocyclic gp120 inhibitors by reducing the distance between the important pharmacophores namely, Phe and Arg on the *m* side of the most potent backbone cyclic inhibitor C-2-2.

In order to reduce the size of the potential HIV-1 inhibitors, three amino acids from the Phe region (Gln40, Gly41, and Ser42) were replaced with a diamide linker (pimelic acid). Furthermore, since the proximity of the Arg and Phe pharmacophores is critical for the anti HIV-1 activity, we decided to shorten the distance between these two crucial pharmacophores. The distance between the Arg guanidine and the Phe aromatic moiety in C-2-2 is 12 atoms. By inserting the guanidine or the phenylic moiety as part of the bridge methylene linker the distance between the two functional groups could be shorten to only nine atoms (Scheme 2). Three small molecules, CG-1, SC-1, and MC-1, with molecular weights of about 500 g/mol were synthesized on solid support. The three molecules share a similar scaffold comprising fourteen atoms in the ring and the same chirality of the side chains.

As described in Scheme 2, all macrocyclic scaffolds were constructed using similar synthetic steps. The most challenging step was the on-resin reductive amination. Three aldehydes were syn-

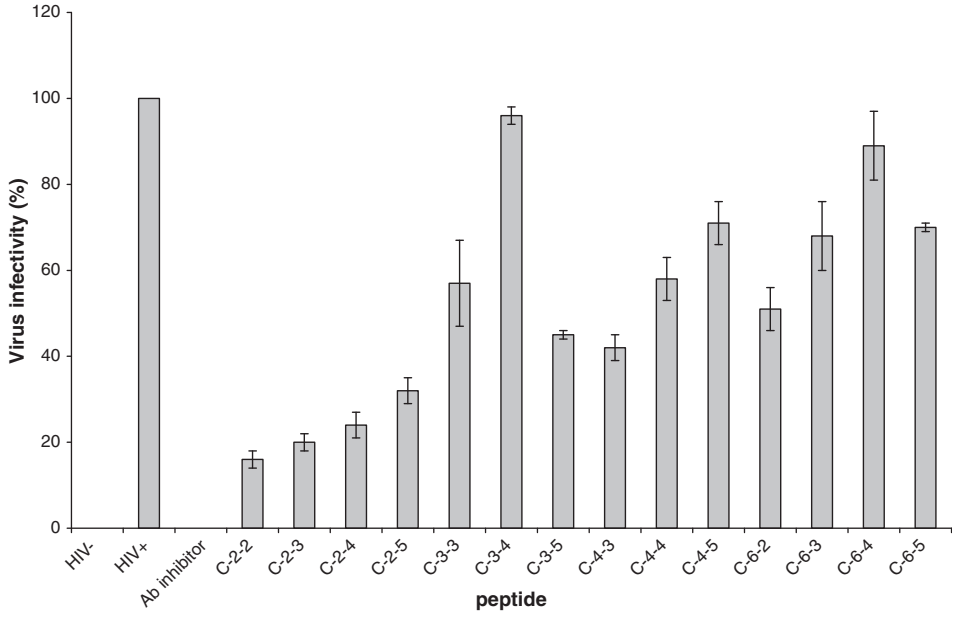

Figure 2. Inhibition of viral infectivity by C-*n*-*m* peptides.

thesized in solution (see Supplementary data). Aldehydes Fmoc-L-Arg(Alloc)$_2$-H and Alloc-L-Tyr(*t*-Bu)-H were produced by oxidation of the corresponding alcohols using Dess–Martin periodinane as described previously.[16,17] Alloc-L-Phe-H was prepared by reduction of the corresponding Weinreb amide as described.[18,19]

The alpha nitrogen of Rink-amide 4-methylbenzhydrylamine (MBHA) resin bound glycine was treated with the above aldehydes and reduced with $NaCNBH_3$ to give the corresponding secondary amine. A protected amino acid was coupled to the obtained secondary amine using either *bis*(trichloromethyl)carbonate (BTC) or 2-(7-aza-1*H*-benzotriazole-1-yl)-1,1,3,3-tetramethyluronium hexafluorophosphate (HATU) as coupling reagent. The use of milder reagents proved insufficient for complete coupling. After coupling, the temporary protecting groups (Fmoc on MC-1, Boc on SC-1 and allyloxycarbonyl (Alloc) on CG-1) were removed. Selective Boc deprotection in the synthesis of SC-1 was a challenge. Boc is commonly used as permanent protection in Fmoc based solid phase synthesis and its removal was considered as nonorthogonal to the appropriate resin. Sivanandaiah et al. reported iodotrichlorosilane as an efficient agent for Boc deprotection.[20] However, this method proved too cumbersome to be used routinely and was abandoned after few attempts. We have used a recently published procedure described by Freeman and Gilon for the selective removal of Boc from peptide-bound to Rink-amide MBHA resin. This procedure proved to be mild enough to allow selective Boc removal without major reduction in overall yield.[21] Pimelic acid was attached to the primary amine using *N*,*N*′-diisopropylcarbodiimide (DIC) for activation. The second temporary protecting group was removed according to standard procedures (Alloc for MC-1, Fmoc for CG-1 and SC-1). However, incomplete Fmoc removal from the Arg moiety in CG-1 synthesis using standard conditions occurred. We have used the more reactive base, 1,8-diazabicyclo[5.4.0] undec-7-ene (DBU), to ensure complete removal of Fmoc before the cyclization step. Cyclization was performed using the new coupling reagent 6-chloro-benzotriazole-1-yl-oxy-tris-pyrrolidino-phosphonium hexafluorophosphate (PyClock). For MC-1 and CG-1 a simple cleavage procedure was used for consecutive removal of the remaining semi-permanent protecting groups and the macrocycles from the resin. For SC-1, Alloc removal from the guanidine moiety was performed prior to cleavage. The macrocyclic scaffolds synthesized here possess an active pharmacophore as part of the cyclization bridge.

We report an extension of works previously published that introduce functional linkers by on-resin reductive amination procedure.[16,22,23] Utilizing these methods we were able to synthesize the macrocycles on solid support. Adopting these methods minimize the amount of synthetic steps involved in precursors' preparation.

Previous studies demonstrated that the role of CD4 Phe43 is crucial for gp120 binding and its replacement with other amino acids including tyrosine resulted in dramatic decrease in binding ability.[12] To test whether CG-1 binds gp120 in the same manner as CD4, we replaced the phenyl moiety in CG-1 with a phenol. The resulting molecule, MC-1, has exactly the same scaffold, structure and pharmacophores topology as CG-1 but possesses a hydroxyl on the para position of the phenyl moiety replacing hydrogen.

2.3. Biological activity of small molecule macrocyclic HIV-1 infection inhibitors

The effect of MC-1, SC-1, and CG-1 on HIV-1 propagation was studied. We showed that MC-1 did not reduce the infectivity of HIV-1 in cultured cells at the μM range (Fig. 3A). This indicates that the CD4:gp120 interaction was not interrupted by MC-1. This agrees with previous results, suggesting that the addition of the hydroxyl group to Phe43 on CD4 disrupts low energy interactions with the gp120 hydrophobic pocket. The mechanism for CD4:gp120 interaction inhibition by small molecules is still unclear. While it is possible that the inhibitors occupy the Phe43 pocket, X-ray studies suggest a Water-filled channel as an alternative binding site for these inhibitors.[24] Furthermore, inhibitors like T-20 disrupt the interaction by imposing allosteric changes to the envelope protein and not by occupation of the interaction site. Preliminary docking experiments suggest that CG-1 fit the Phe43 pocket. However, the conformational changes gp120 experiences during binding put in doubt any design and development based solely on the X-ray structure of the complex.[25] Although our results imply that CG-1 binds gp120 at the Phe43 pocket this point will be further investigated by in vitro studies.

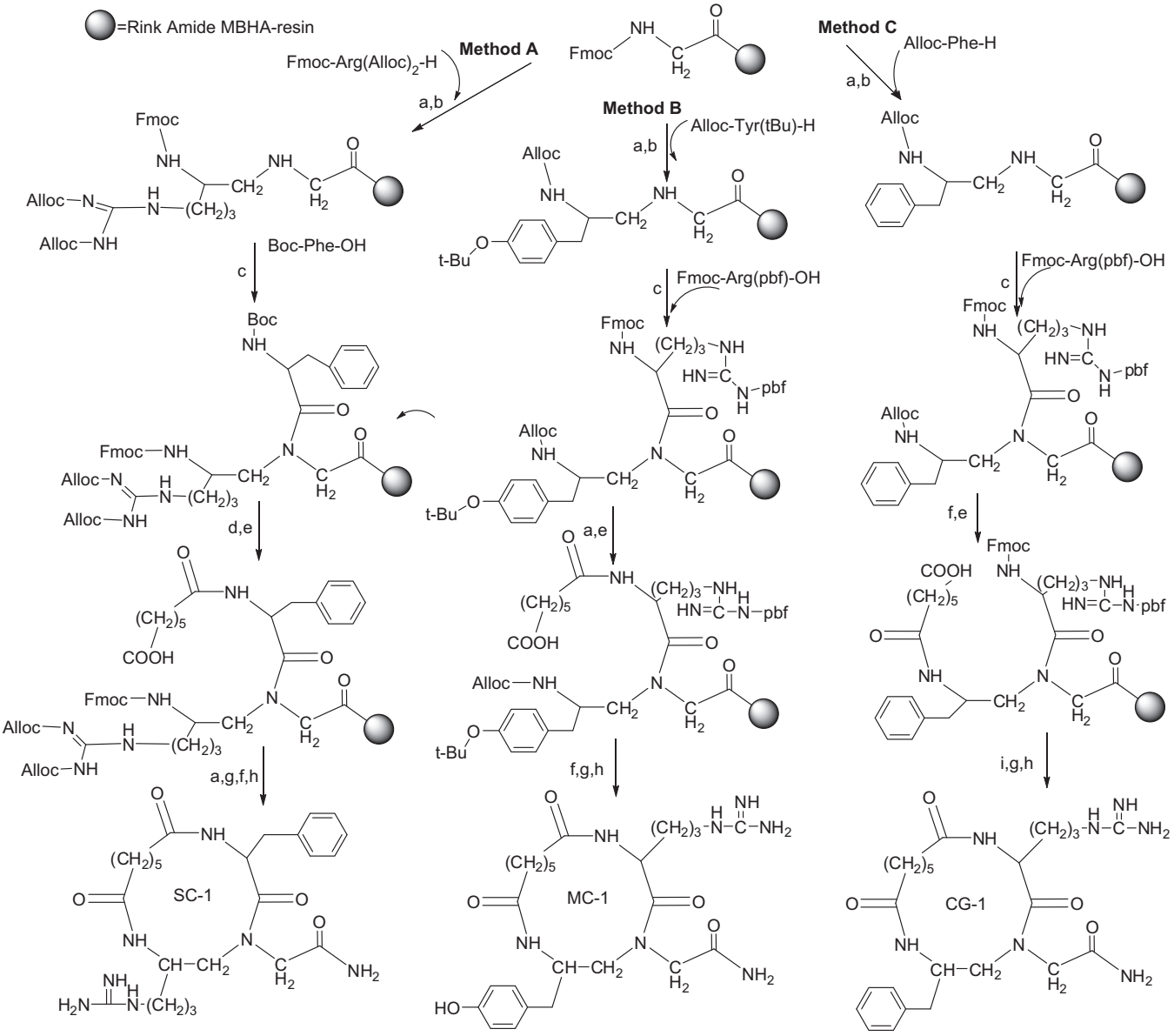

Scheme 2. Synthesis of the macrocyclic CD4 mimetics. Reagents and conditions: (a) piperidine; (b) Alloc-L-Tyr(*t*-Bu)-H or Boc-L-Phe-H or Fmoc-L-Arg(Alloc)$_2$-H, $NaCNBH_3$; (c) Boc-L-Phe-OH or Fmoc-L-Arg(pbf)-OH, HATU, HOAt, DIPEA; (d) 0.05 M $SnCl_4$; (e) pimelic acid, DIC, DMAP; (f) $Pd(PPh_3)_4$, AcOH, *N*-methylmorpholine; (g) PyClock, DIPEA; (h) TFA, TDW, TIPS; (i) 10% DBU.

CG-1 and SC-1 are structural regioisomers having the same scaffold that preserve the original CD4 active pharmacophores but differ in the position of the functional groups (Scheme 2). While SC-1 shows only weak inhibitory effect on HIV-1 infection (inhibits virus infection in the high μM range), CG-1 inhibits more then 80% of viral infection in the low μM range. The difference between the CG-1 and SC-1 isomers in HIV-1 infection inhibition indicates that the potency is dictated not only by the nature of the pharmacophores but also influenced by the correct orientation of the active moieties. The effect of CG-1 on virus infection was studied (Fig. 3B) by three independent assays that reaffirmed in a concentration dependent manner that CG-1 has low μM activity.

In 2004, Dahno et al. evaluated the reasonable size for drug candidates that aim to block transmembrane proteins interaction.[14] The work was based on several commercially available drugs and suggests that the optimal distance between the important residues is 10–15 Å. CG-1 size falls well within this criteria and has drug-like structure and characteristics.

We further evaluated its potential as drug candidate by studying its oral bioavailability properties.

2.4. Pharmacokinetic parameters following IV and PO administration

The pharmacokinetic profile of CG-1 was studied by following intravenous (IV) and per os (PO) administration to rats (presented in Fig. 4). The pharmacokinetic parameters derived from administration of CG-1 to rats are depicted in Table 1.

CG-1 half-life was about 73 min. This is a relatively long half-life in comparison to native peptides. This finding reaffirm previous reports that indicate that chemical modification (arise from cyclization) resulted in a metabolically stable macrocyclic molecule.

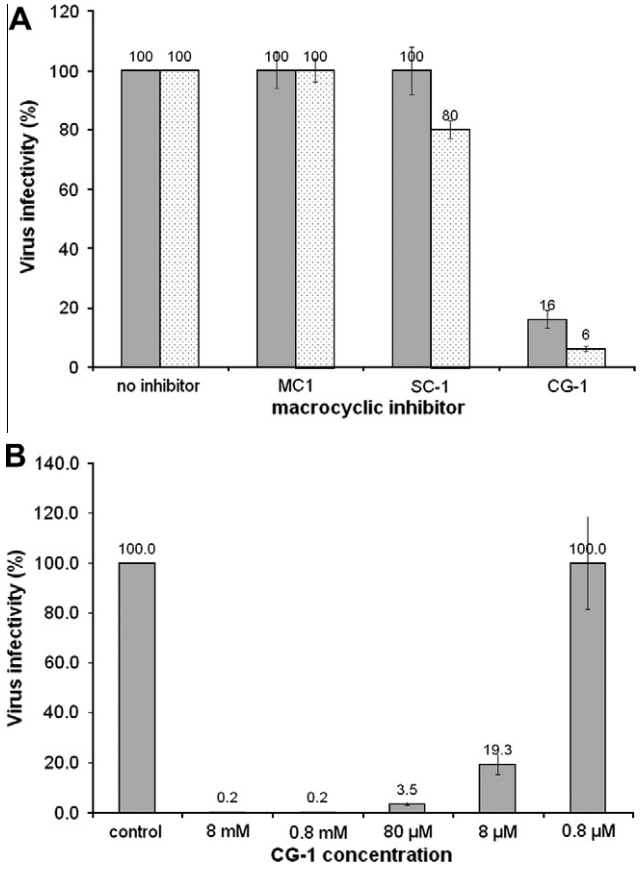

Figure 3. CG-1 blocks HIV-1 infection in MAGI HeLa cells. (A) Inhibition of HIV-1 infection was evaluated following treatment with 10 μM (grey) and 1 μM (dots) of MC-1, SC-1, and CG-1. (B) CG-1 inhibits HIV-1 infection in a concentration dependent manner.

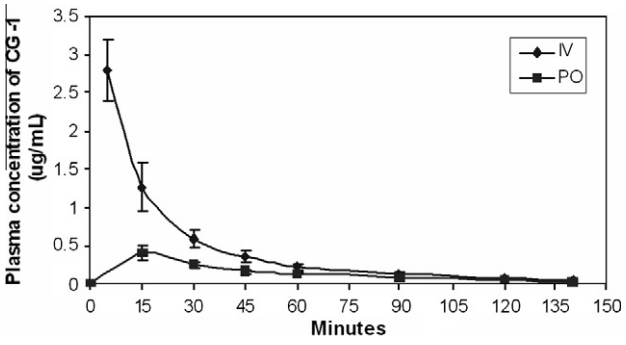

Figure 4. Plasma concentrations of CG-1 were plotted against time scale after IV bolus and PO administration to conscious Wistar rats, $n = 5$ in each group, values are average ± SEM.

The calculated oral bioavailability (10%) further strengthened our preliminary findings of good ex-vivo permeability. The relatively high volume of distribution (Vss: 0.6 L/kg) provides an indirect indication of the restricted ability to cross biological membranes.

3. Conclusion

Backbone cyclization and macrocyclization is presented here as rational methods to mimic noncontinuous active regions in transmembrane proteins aimed to inhibit protein–protein interaction. Screening a small set of backbone cyclic peptides enabled a detection of a structure activity relationship pattern that was used to design a small macrocyclic inhibitor. We applied this concept to the HIV-1 CD4:gp120 model, and showed that the active site in CD4 can be minimized. Furthermore, the screening of backbone cyclic peptide library proved useful in the design of macrocyclic HIV-1 inhibitors that can mimic the CD4 active site.

The unique protecting group manipulation and, in particular, the novel orthogonal Boc deprotection procedure used here was essential for the synthesis of the scaffolds and can be adopted as strategy for the preparation of other molecules on solid support. CG-1 inhibits viral infection in cells in the low micromolar range and has good pharmacological properties, for example, oral bioavailability. We claim that CG-1, having the combined properties of inhibitory effect, high stability and superior oral bioavailability, is an attractive lead for further drug development. We also claim that by adapting the approach presented here active regions in other protein binding sites can be minimized to drug-like molecules.

4. Experimental section

4.1. Chemistry general

All starting materials were purchased from commercial sources and were used without further purification. Nuclear magnetic resonance (NMR) spectra during synthesis were recorded on a Bruker AMX 300, Bruker 400 or Bruker 500 MHz spectrometer. Chemical shifts are reported downfield, relative to internal solvent peaks. Coupling constants *J* are reported in Hz. High Resolution Mass spectrometry (HRMS) spectra were recorded on nanospray ionization LTQ orbitrap. Matrix assisted laser desorption ionization (MALDI)-time of flight (TOF) (MALDI-TOF) Mass spectra were recorded on a PerSeptive Biosystems MALDI-TOF MS, using α-cyano-4-hydroxycinnamic acid as matrix. Thin layer chromatography (TLC) was performed on Merck aluminum sheets silica gel 60 F254. Column chromatography was performed on Merck silica gel 60 (230–400 mesh). Peptides purification: Peptides purity was determined by analytical HPLC, peptides below 95% purity were excluded from further examination (see Supplementary data). Analytical HPLC was performed on Vydac analytical columns (C18, 5 μm, 4.6 mm × 250 mm (218TP54)) using Merck–Hitachi system: Model LaChrom with a L-7100 pump, L-7200 autosampler, L-7400 UV–Vis detector and a D-7000 interface. Products were assayed at 215 and 220 nm. The mobile phase consisted of a gradient system, with solvent A corresponding to TDW with 0.1% TFA and solvent B corresponding to acetonitrile (ACN) with 0.1% TFA. The mobile phase started with 95% A from 0 to 5 min followed by a linear gradient from 5% B to 95% B from 5 to 55 min. The gradient remained at 95% B for an additional 5 min and then was reduced to 95% A and 5% B from 60 to 65 min. The gradient remained at 95% A for additional 5 min to achieve column equilibration. The flow rate of the mobile phase was 1 mL/min. Peptide purification was performed by reversed

Table 1
Pharmacokinetic properties of CG-1 after administration to Wistar rats

PK parameters	C_{max} (ng/mL)	T_{max} (min)	AUC (min × ng/mL)	Cl (mL/min/kg)	Vss (L/kg)	$T_{1/2}$ (min)[a]	Oral bioavailability[a]
PO	866 ± 76	18	21770 ± 63	14.53 ± 0.33	0.6	73	~10%
IV	102 ± 19	5					

[a] Noncompartmental pharmacokinetic analysis was performed using WinNonlin software, standard.

phase semi-preparative HPLC on a Merck–Hitachi 665A model equipped with a preparative pump (30 mL/min) and a high flow UV–Vis detector using semi-preparative Vydac column (C18, 5 μm, 10 × 250 (208TP510)) flow rate of the mobile phase was 4.5 mL/min. All semi-preparative HPLC runs were carried out using a gradient system similar to the one used in for the analytical HPLC. Macrocycles purification: Analytical RP-HPLC were recorded at 220 nm at a flow of 1 mL/min on Merck–Hitachi system (LaChrom with a L-7100 pump, L-7200 autosampler, L-7400 UV–Vis detector and a D-7000 interface) on Phenomenex RP-18 column (C18, 5 μ, 4.6 × 75 mm (Luna)). Using the same solvent system previously described, the mobile phase started with 95% A from 0 to 5 min followed by a linear gradient from 5% B to 95% B from 5 to 17 min. The gradient remained at 95% B for an additional 4 min and then was reduced to 95% A from 21 to 25 min. The gradient remained at 95% A for additional 5 min to achieve column equilibration. Semi-preparative HPLC were recorded at 220 nm on Phenomenex RP-18 column (C18, 10 μ 250 × 10 mm, 110 Å (Gemini)). Using the same solvent system previously described, the mobile phase started with 95% A from 0 to 5 min followed by a linear gradient from 5% B to 35% B from 5 to 30 min, then to 95% B in 15 min, the gradient remained at 95% B for an additional 5 min and then was reduced to 95% A in 10 min. The gradient remained at 95% A for additional 5 min to achieve column equilibration.

4.2. Peptide synthesis

Backbone cyclic peptides were named systematically C-*n*-*m* where *n* describe the number of methylenes in the building unit and *m* represents the number of methylenes in the linker (Scheme 1). The Peptides were synthesized on methylbenzhydrylamine (MBHA) resin using the combinatorial 'tea bag' method[10] using Fmoc and Boc chemistries as described before.[1,11] Final cleavage was performed using HF/anisole mixture or by trimethylsilyl trifluoromethane sulfonate/anisole/trifluoroacetic acid mixture. Out of the designed peptide library thirteen were prepared in sufficient yield and purity to allow biological screening (Table 1).

4.3. General methods for solid phase synthesis of macromolecules C

Swelling: The resin was swelled for at least 2 h in DCM. Fmoc removal: The resin was treated with a solution of 20% piperidine in NMP (2 × 20 min), and then washed with NMP (5 × 2 min). HBTU coupling: Protected amino acids (1.5 equiv) were dissolved in NMP. *N*,*N*-Diisopropylethylamine (DIPEA) (1.5 equiv) and 1-hydroxybenzotriazole (HOBt) (1.5 equiv) were added and the mixture was cooled to 0 °C. (2-(1*H*-Benzotriazole-1-yl)-1,1,3,3-tetramethyluronium hexafluorophosphate) (HBTU) (1.5 equiv) was added and the mixture was pre-activated by mixing for 10 min, added to the resin, and shaken for 1 h. The resin was washed with NMP (3 × 2 min). Capping: The resin was treated with a solution of AC_2O (10 equiv) and DIPEA (7.15 equiv) in DMF for 20 min and washed with NMP (3 × 2 min). HATU coupling: Fmoc protected amino acids (1.5 equiv) were dissolved in NMP, DIPEA (1.5 equiv) and 1-hydroxy-7-aza-benzotriazole (HOAt) (1.5 equiv) were added and the mixture was cooled to 0 °C. (2-(7-Aza-1*H*-benzotriazole-1-yl)-1,1,3,3-tetramethyluronium hexafluorophosphate) (HATU) (1.5 equiv) was added and the mixture was pre-activated by mixing for 10 min, added to the resin, and shaken overnight at rt. The resin was washed with NMP (3 × 2 min).

4.3.1. Solid-phase synthesis SC-1: method A

Fmoc-Rink-amide MBHA resin was washed with NMP and left 2 h for swelling. Fmoc group was removed using 20% piperidine solution and then resin was washed with NMP (3 × 5 min). Fmoc-Gly-OH was coupled using HBTU activation followed by washing with NMP (3 × 5 min). The Fmoc group was removed, and the resin was washed with NMP (3 × 5 min). Fmoc-L-Arg(Alloc)$_2$-CHO (4 equiv), dissolved in NMP/MeOH solution containing 1% AcOH, was added to the resin followed by the addition of $NaBH_3CN$ (4 equiv) and left to stir for 4 h. Resin was washed with NMP/MeOH (1 × 5 min), MeOH (1 × 5 min), 1% AcOH/water (1 × 5 min), 10% water in MeOH (1 × 5 min), MeOH (1 × 5 min), NMP (1 × 5 min), DCM (1 × 5 min), and NMP (3 × 5 min). Boc-L-Phenylalanine-OH was coupled using HATU activation overnight followed by washing with NMP (3 × 5 min). Boc was removed using the recently published procedure.[21] Resin was treated with 0.05 M $SiCl_4$ in DCM (dry) (2 × 15 min) followed by washing with DCM (1 × 5 min), DMF (1 × 5 min), 20% MeOH/DMF (1 × 5 min), 1% DIPEA/DMF (2 × 5 min), and NMP (3 × 5 min). Pimelic acid (10 equiv) was pre-activated with DIC (10 equiv) in NMP and was added to the resin followed by addition of 4-(Dimethylamino)pyridine (DMAP) (1 equiv) left for 3 h then washed with NMP (3 × 5 min). The Fmoc group was removed, resin was washed with NMP (3 × 5 min) then treated with a solution of PyClock (6 equiv) and DIPEA (14 equiv) in NMP for 4 h (×2). Resin was washed with NMP (2 × 5 min), DCM (2 × 5 min), and MeOH (2 × 5 min) then dried under vacuum. Resin was treated with $Pd(PPh_3)_4(0)$ (1:1 weight equiv) in NMM/AcOH/DCM(dry)(2.5/2.5/95%) solution for 2 h in dark then washed with 0.5% DIPEA in NMP (3 × 5 min), 0.5% sodium diethyldithiocarbamate trihydrate in NMP (5 × 2 min), NMP (2 × 2 min), DCM (2 × 2 min), MeOH (2 × 2 min), and dried in vacuum. Crude was cleaved from the resin by treatment with TFA/triisopropylsilane (TIPS)/TDW (92.5/5/2.5%) solution for 2.5 h. The solution was separated by filtration and the resin was rinsed with neat TFA. The TFA was evaporated to give crude oil that was dissolved in ACN:TDW 1:1 solution and lyophilized. Crude was purified on semi-preparative HPLC as described above, collected peaks were analyzed using analytical HPLC and pure compounds (over 95% purity were used for biological screening).

SC-1: Prepared from 200 mg of Fmoc-Rink MBHA resin. Yield: 0.8 mg. HPLC purity >95%. Rt 9.73. HRMS (Orbitrap-ESI): exact mass calcd for C24H38N7O4 488.2980 (MH^+). Found 488.2968.

4.3.2. Solid-phase synthesis MC-1: method B

Fmoc-Rink-amide MBHA resin was washed with NMP and left 2 h for swelling. Fmoc group was removed and resin was washed with NMP (3 × 5 min). Fmoc-Gly-OH was coupled using HBTU activation followed by washing with NMP (3 × 5 min). The Fmoc group was removed and resin was washed with NMP (3 × 5 min). Alloc-L-Tyr(*t*-Bu)-CHO (4 equiv) in 1% AcOH in NMP/MeOH was added to the resin followed by the addition of NaBH3CN (4 equiv) and left to stir for 4 h. Resin was washed with NMP/MeOH (1 × 5 min), MeOH (1 × 5 min), 1% AcOH/water (1 × 5 min),10% water in MeOH (1 × 5 min), MeOH (1 × 5 min), NMP (1 × 5 min), DCM (1 × 5 min), and NMP (3 × 5 min). Fmoc-L-Arg(2,2,4,6,7-pentamethyldihydrobenzofuran-5-sulfonyl (pbf))-OH was coupled using HATU activation overnight followed by washing with NMP (3 × 5 min). Fmoc group was removed and resin was washed with NMP (3 × 5 min). Pimelic acid (10 equiv) was pre-activated with DIC (10 equiv) in NMP and was added to the resin followed by addition of DMAP (1 equiv) left for 3 h. Resin was washed with NMP (2 × 5 min), DCM (2 × 5 min), and MeOH (2 × 5 min) then dried under vacuum. Alloc was removed by treatment with $Pd(PPh_3)_4(0)$ (0.5 equiv) in NMM/AcOH/DCM(dry)(2.5/2.5/95%) solution for 2 h in dark, then washed with 0.5% DIPEA in NMP (3 × 5 min), 0.5% sodium diethyldithiocarbamate trihydrate in NMP (5 × 2 min), NMP (2 × 2 min), DCM (2 × 2 min), MeOH (2 × 2 min), and dried in vacuum. The Fmoc group was removed, resin was washed with NMP (3 × 5 min) then treated with a solution of PyClock (6 equiv) and

DIPEA (14 equiv) in NMP for 4 h (×2). Resin was washed with NMP (2 × 5 min), DCM (2 × 5 min), and MeOH (2 × 5 min) then dried under vacuum. Crude was cleaved from the resin by treatment with TFA/TIPS/TDW (92.5/5/2.5%) solution for 2.5 h. The solution was separated by filtration and the resin was rinsed with neat TFA. The TFA was evaporated to give crude oil that was dissolved in ACN:TDW 1:1 solution and lyophilized. Crude was purified on semi-preparative HPLC as described above, collected peaks were analyzed using analytical HPLC and pure compounds (over 95% purity were used for biological screening).

MC-1: Prepared from 200 mg of Fmoc-Rink MBHA resin. Yield: 1.4 mg. HPLC purity >95%. Rt 8.79. HRMS (Orbitrap-ESI): exact mass calcd for C24H38N7O5 504.2929 (MH^+). Found 504.2919.

4.3.3. Solid-phase synthesis CG-1: method C

Fmoc-Rink-amide MBHA resin was washed with NMP and left 2 h for swelling. The Fmoc group was removed and resin was washed with NMP (3 × 5 min). Fmoc-Gly-OH was coupled using HBTU activation followed by washing with NMP (3 × 5 min). The Fmoc group was removed and resin was washed with NMP (3 × 5 min). Alloc-L-Phe-CHO (4 equiv) in 1% AcOH in NMP/MeOH was added to the resin followed by the addition of $NaBH_3CN$ (4 equiv) and left to stir for 4 h. Resin was washed with NMP/MeOH (1 × 5 min), MeOH (1 × 5 min), 1% AcOH/water (1 × 5 min), 10% water in MeOH (1 × 5 min), MeOH (1 × 5 min), NMP (1 × 5 min), DCM (1 × 5 min), and NMP (3 × 5 min). Fmoc-L-Arg(pbf)-OH was coupled using HATU activation overnight followed by washing with NMP (3 × 5 min), DCM (2 × 5 min), and MeOH (2 × 5 min) then dried under vacuum. Alloc was removed by treatment with $Pd(PPh_3)_4(0)$ (0.5 equiv) in NMM/AcOH/DCM(dry)(2.5/2.5/95%) solution for 2 h in dark, then washed with 0.5% DIPEA in NMP (3 × 5 min), 0.5% sodium diethyldithiocarbamate trihydrate in NMP (5 × 2 min), NMP (2 × 2 min), DCM (2 × 2 min), MeOH (2 × 2 min), and NMP (2 × 3 min). Pimelic acid (10 equiv) was pre-activated with DIC (10 equiv) in NMP and was added to the resin followed by addition of DMAP (1 equiv) left for 3 h, then washed with NMP (3 × 5 min) and the Fmoc group was removed using a solution of 10% 1,8-diazabicyclo[5.4.0]undec-7-ene (DBU) in NMP (2 × 1/2 h). The resin was washed with NMP (3 × 5 min) then treated with a solution of PyClock (6 equiv) and DIPEA (14 equiv) in NMP for (2 × 4 h). The resin was washed with NMP (2 × 5 min), DCM (2 × 5 min), and MeOH (2 × 5 min) then dried under vacuum. Crude was cleaved from the resin by treatment with TFA/TIPS/TDW (92.5/5/2.5%) solution for 2.5 h. The resin was filtered and rinsed with neat TFA. The TFA solution was evaporated to give a crude oil that was dissolved in acetonitrile:TDW 1:1 solution and lyophilized. The crude product was purified on semi-preparative HPLC as described above, collected peaks were analyzed using analytical HPLC and pure compounds (over 95% purity) were used for biological screening.

CG-1: Prepared from 200 mg of Fmoc-Rink MBHA resin. Yield: 1.2 mg (2.1%). Analytical HPLC purity >95%. Rt 9.71. HRMS (Orbitrap-ESI): exact mass calcd for C24H38N7O4 488.2980 (MH^+). Found 488.2976.

4.3.4. HIV-1 titration

Titration of HIV-1 strand HXB2 in the absence or presence of the inhibitor was carried out by the multinuclear activation of a galactosidase indicator (MAGI) assay, as described by Kimpton and Emerman.[15] Briefly, HeLa−CD4+beta-gal cells were transferred into 96-well plates at 15×10^3 cells per well. On the following day, the cells were infected with 50 μL of serially diluted virus in the presence of 20 mg/mL of DEAE-dextran (Pharmacia, Sweden). Two days post-infection, cultured cells were fixed with 1% formaldehyde and 0.2% glutaraldehyde in PBS. Following intensive wash with PBS, cells were stained with a solution of 4 mM potassium ferrocyanide, 4 mM potassium ferricyanide, 2 mM $MgCl_2$ and 0.4 mg/mL of X-Gal (Ornat, Israel). Blue cells were counted under a light microscope.

4.3.5. Animals

Male Wistar rats (275 ± 20 g) were purchased from Harlan laboratories (Rehobot, Israel). Rats were kept in a light-controlled room (light from 7:00 to 19:00) and were maintained on laboratory chow and water ad libitum.

All surgical and experimental procedures were reviewed and approved by the Animal Experimentation Ethics Committee of the Hebrew University Hadassah Medical Center, Jerusalem.

4.3.6. Pharmacokinetic study

Studies were performed in conscious Wistar male rats. An indwelling cannula was implanted into the left jugular vein 24 h before the pharmacokinetic experiment to allow full recovery of the animals from the surgical procedure. Animals ($n = 5$) received an intravenous (IV) bolus dose of 1 mg/kg of CG-1 or 10 mg/kg by oral gavage ($n = 5$), CG-1 was dissolved in water. Blood samples (with heparin, 15 U/mL) were collected at several time points up to 24 h after CG-1 administration. Plasma was separated by centrifugation (4000 g, 5 min, 4 °C) and stored at −70 °C pending analysis. Noncompartmental pharmacokinetic analysis was performed using WinNonlin software, standard

Acknowledgment

The authors like to thank Luxembourg Industries Ltd. for supplying PyClock that was used throughout this work.

Supplementary data

Supplementary data (characterization of C-*n*-*m* library, synthetic procedure of aldehyde preparation, and NMR results) associated with this article can be found, in the online version, at doi:10.1016/j.bmc.2010.04.053.

References and notes

1. Kasher, R.; Oren, D. A.; Barda, Y.; Gilon, C. *J. Mol. Biol.* **1999**, *292*, 421.
2. Gilon, C.; Halle, D.; Chorev, M.; Selinger, Z.; Byk, G. *Biopolymers* **1991**, *31*, 745.
3. Hess, S.; Linde, Y.; Ovadia, O.; Safrai, E.; Shalev, D. E.; Swed, A.; Halbfinger, E.; Lapidot, T.; Winkler, I.; Gabinet, Y.; Faier, A.; Yarden, D.; Xiang, Z.; Portitlo, F. P.; Haskell-Luevano, C.; Gilon, C.; Hoffman, A. *J. Med. Chem.* **2008**, *51*, 1026.
4. Hess, S.; Ovadia, O.; Shalev, D. E.; Senderovich, H.; Qadri, B.; Yehezkel, T.; Salitra, Y.; Sheynis, T.; Jelinek, R.; Gilon, C.; Hoffman, A. *J. Med. Chem.* **2007**, *50*, 6201.
5. Este, J. A.; Telenti, A. *Lancet* **2007**, *370*, 81.
6. Si, Z.; Madani, N.; Cox, J. M.; Chruma, J. J.; Klein, J. C.; Schon, A.; Phan, N.; Wang, L.; Biorn, A. C.; Cocklin, S.; Chaiken, I.; Freire, E.; Smith, A. B., 3rd; Sodroski, J. G. *Proc. Natl. Acad. Sci. U.S.A.* **2004**, *101*, 5036.
7. Zhao, Q.; Ma, L.; Jiang, S.; Lu, H.; Liu, S.; He, Y.; Strick, N.; Neamati, N.; Debnath, A. K. *Virology* **2005**, *339*, 213.
8. Kilby, J. M.; Hopkins, S.; Venetta, T. M.; DiMassimo, B.; Cloud, G. A.; Lee, J. Y.; Alldredge, L.; Hunter, E.; Lambert, D.; Bolognesi, D.; Matthews, T.; Johnson, M. R.; Nowak, M. A.; Shaw, G. M.; Saag, M. S. *Nat. Med.* **1998**, *4*, 1302.
9. Kwong, P. D.; Wyatt, R.; Robinson, J.; Sweet, R. W.; Sodroski, J.; Hendrickson, W. A. *Nature* **1998**, *393*, 648.
10. Brodsky, M. H.; Warton, M.; Myers, R. M.; Littman, D. R. *J. Immunol.* **1990**, *144*, 3078.
11. Kwong, P. D.; Wyatt, R.; Majeed, S.; Robinson, J.; Sweet, R. W.; Sodroski, J.; Hendrickson, W. A. *Structure* **2000**, *8*, 1329.
12. Moebius, U.; Clayton, L. K.; Abraham, S.; Harrison, S. C.; Reinherz, E. L. *J. Exp. Med.* **1992**, *176*, 507.
13. Myszka, D. G.; Sweet, R. W.; Hensley, P.; Brigham-Burke, M.; Kwong, P. D.; Hendrickson, W. A.; Wyatt, R.; Sodroski, J.; Doyle, M. L. *Proc. Natl. Acad. Sci. U.S.A.* **2000**, *97*, 9026.
14. Dahno, W.; Swistok, J.; Khan, W.; Fry, D.; Sun, H.; Falcioni, F.; Goodnow, R., Jr.; Truitt, T.; Hoffman, A.; Garippa, R. In *Third International and Twenty-Eight European Peptide Symposium*; Martin, F., Mati, F., Chaim, G., Jirina, S., Eds.; Kenes International: Prague, Czech Republic, 2004.
15. Kimpton, J.; Emerman, M. *J. Virol.* **1992**, *66*, 2232.

16. Bondebjerg, J.; Xiang, Z. M.; Bauzo, R. M.; Haskell-Luevano, C.; Meldal, M. *J. Am. Chem. Soc.* **2002**, *124*, 11046.
17. Myers, A. G.; Zhong, B. Y.; Movassaghi, M.; Kung, D. W.; Lanman, B. A.; Kwon, S. *Tetrahedron Lett.* **2000**, *41*, 1359.
18. Ede, N. J.; Eagle, S. N.; Wickham, G.; Bray, A. M.; Warne, B.; Shoemaker, K.; Rosenberg, S. *J. Pept. Sci.* **2000**, *6*, 11.
19. Nahm, S.; Weinreb, S. M. *Tetrahedron Lett.* **1981**, *22*, 3815.
20. Sivanandaiah, K. M.; Sureshbabu, V. V.; Shankaramma, S. C. *Int. J. Pept. Protein Res.* **1995**, *45*, 377.
21. Freeman, N. S.; Gilon, C. *Synlett* **2009**, 2097.
22. Hurevich, M.; Barda, Y.; Gilon, C. *Heterocycles* **2007**, *73*, 617.
23. Qvit, N.; Reuveni, H.; Gazal, S.; Zundelevich, A.; Blum, G.; Niv, M. Y.; Feldstein, A.; Meushar, S.; Shalev, D. E.; Friedler, A.; Gilon, C. *J. Comb. Chem.* **2008**, *10*, 256.
24. Madani, N.; Perdigoto, A. L.; Srinivasan, K.; Cox, J. M.; Chruma, J. J.; LaLonde, J.; Head, M.; Smith, A. B., 3rd; Sodroski, J. G. *J. Virol.* **2004**, *78*, 3742.
25. Caporuscio, F.; Tafi, A.; Gonzalez, E.; Manetti, F.; Este, J. A.; Botta, M. *Bioorg. Med. Chem. Lett.* **2009**, *19*, 6087.